Nonisotropic Enzyme−Inhibitor Interactions: A Novel Nonoxidative Mechanism for Quantum Proteolysis by Human Neutrophils†

Theodore G. Liou‡ and Edward J. Campbell*,‡,§,||

Division of Respiratory, Critical Care, and Occupational Pulmonary Medicine, Department of Medicine, University of Utah Health Sciences Center, Salt Lake City, Utah 84132, and Salt Lake City Veterans Administration Medical Center, Salt Lake City, Utah 84148

Received May 19, 1995; Revised Manuscript Received August 14, 1995⊗

ABSTRACT: Traditional theories of enzyme kinetics do not model the influences of rapidly changing and nonisotropic enzyme concentrations in real-world systems. We have modeled local enzyme concentrations in space and time following quantal release of human leukocyte elastase (HLE) from cytoplasmic granules of polymorphonuclear neutrophils (PMN). Calculations from first principles indicate that ~67 000 molecules of HLE are stored in each azurophil granule at a mean concentration of 5.33 mM, which exceeds pericellular inhibitor concentrations *in vivo* by nearly 3 orders of magnitude. Diffusion analysis predicts obligate catalytic activity (excess of local enzyme over inhibitor concentration) that extends to 1.33 μm from the site of granule extrusion (7.8-fold larger than the mean radius of the granule), with a duration of 12.4 ms, when the pericellular concentration of α_1-antitrypsin equals that of normal plasma. In contrast, when PMN are bathed in α_1-antitrypsin concentrations found in plasma from individuals with α_1-antitrypsin deficiency, the radius and duration of obligate catalytic activity are increased 2.5-fold and 6.2-fold, respectively. These simulations agree remarkably well with our recent direct observations and provide a novel, nonoxidative mechanism by which quantum bursts of extracellular proteolytic activity occur despite proteinase inhibitors in the bathing medium. Titration of local enzyme−inhibitor concentration is the dominant determinant of the size and duration of such events. This construct provides new insights into the pathogenesis of tissue injury in α_1-antitrypsin deficiency. The nonisotropic analyses presented herein supplement Michaelis−Menten theory and have implications for the pathogenesis and therapy of α_1-antitrypsin deficiency and other inflammatory diseases associated with considerable morbidity and mortality.

Traditional analyses of enzyme kinetics are constrained to well-stirred systems. The inhomogeneity of reactants in real-world systems, however, creates a wealth of complexity in which biochemical reactions can be driven by dynamically changing reactant concentrations that are not anticipated or solved by isotropic models such as Michaelis−Menten kinetics. Ideally, a general model of enzyme−substrate and enzyme−inhibitor interaction would consider the dynamically changing concentrations of all of the reactants in all areas of the system of interest. Inroads into the development of a general theory, however, could be made by modeling the concentration of a principal reactant that varies considerably in space and time.

Certain activities of human inflammatory cells depend upon enzyme−inhibitor systems that have great importance for biology and medicine, and that by their very nature are markedly nonisotropic. For example, in human polymorphonuclear neutrophils (PMN),[1] various proteolytic enzymes are contained within cytoplasmic granules that can be extruded into the extracellular space upon activation of the cells. The concentrations of these enzymes *in vivo* can be expected to change by orders of magnitude with time and distance from the site of release at the cell surface. While experiments in isotropic solution have provided much information about the substrate specificities, catalytic mechanisms, and kinetics of catalysis and inhibition of the proteolytic enzymes released from these cells (Havemann & Janoff, 1978; Bieth, 1986; Owen & Campbell, 1995), isotropic experiments cannot answer critically important questions about mechanisms of catalysis by such enzymes *in vivo*. It is especially noteworthy that Michaelis−Menten kinetics do not model these dynamics and have been inadequate to explain the observed phenomenon of local protein degradation by inflammatory cells despite the presence of large quantities of high-affinity proteinase inhibitors in the pericellular milieu. We hypothesized that a nonisotropic model would not only provide a superior fit to these real-world conditions, but that it could also provide the basis for a nonoxidative mechanism to explain paradoxically uninhibited catalytic activity of proteinases in the microenvironment immediately surrounding PMN (Campbell & Campbell, 1988; Rice & Weiss, 1990).

† This work was supported by USPHS Grants HL46440, HL08938, and HL07636, the Council for Tobacco Research, U.S.A., Inc., and the Department of Veterans Affairs.

* To whom correspondence should be addressed. Phone: (801) 581-7806. FAX: (801) 585-3355.

‡ University of Utah Health Sciences Center.

§ Salt Lake City VAMC.

|| E.J.C. is a Clinical Investigator of the Department of Veteran Affairs.

⊗ Abstract published in *Advance ACS Abstracts,* November 15, 1995.

[1] Abbreviations: a, mean radius of an azurophil granule; C, concentration; C_0, initial concentration; D, diffusion coefficient; HLE, human leukocyte elastase; I_0, modified Bessel function of the first kind, order zero; PMN, human polymorphonuclear neutrophils; r, radius; R, universal gas constant; ρ, density; $s^0_{20,w}$, reduced sedimentation coefficient, 20 °C, water; t, time; V, specific volume.

0006-2960/95/0434-16171$09.00/0

Following quantal release of small amounts of enzyme at high concentrations into inhibitor-containing fluid at the cell surface, "obligate" catalytic activity of the enzyme *must* be present until the molar ratio of enzyme:inhibitor falls to <1:1. Our recent imaging experiments have indicated the need for a nontraditional model for understanding interactions of human leukocyte elastase (HLE) with inhibitor(s) in the pericellular milieu during inflammation (Liou and Campbell, submitted for publication). Moreover, these direct observations have provided a unique opportunity to test predictions derived from nonisotropic enzyme−inhibitor modeling.

Herein, we present a diffusion-based construct that provides a rigorous method for modeling and predicting the behavior of this and similar nonisotropic systems, and that yields a remarkably good fit to observational data. The present analysis also provides insights into the pathogenesis of tissue injury in α_1-antitrypsin deficiency (Hutchison, 1988; Hubbard & Crystal, 1991), the most prevalent potentially lethal hereditary disease of adult Caucasians (Silverman et al., 1989; Troyer et al., submitted for publication).

EXPERIMENTAL PROCEDURES AND RESULTS

HLE is released from PMN at the cell surface and diffuses into the pericellular environment following extrusion of azurophil granules. To model local HLE concentrations, it is first necessary to calculate certain physical parameters of azurophil granules, as well as intragranular HLE concentrations.

Azurophil Granule Volume. Ultrastructural studies have demonstrated that azurophil granules in PMN are elliptical in cross section, with a ratio of long to short axis of 1.3 and an area of 0.1 μm^2 (Damiano et al., 1988). From these data and the formula for the area of an ellipse [$A = \pi$(long axis) × (short axis)], the long and short axes are 203 and 156 nm. We assumed that each granule is an ellipsoid in three dimensions with axes a, b, and c of 203, 156, and 156 nm, respectively (geometric mean radius = 171 nm). From the ellipsoid volume formula [$V = {}^4/_3\pi(abc)$], the volume of a single azurophil granule is 2.09×10^{-17} L.

HLE Concentration in Azurophil Granules. PMN contain 1.11 ± 0.11 (SD) pg of HLE per cell (Campbell et al., 1989). This enzyme is packaged into 399 ± 20 (SEM) azurophil granules (Damiano et al., 1988), each with a volume of 2.09×10^{-17} L. Thus, each granule contains 2.78 fg of HLE (67 000 molecules), at a mean concentration of 5.33 mM.

Calculation of Diffusion Coefficient of HLE. We rearranged the Svedberg equation $D = RTs/M(1 - V\rho)$ (Svedberg & Pedersen, 1940) to calculate the diffusion coefficient, D, in water (ρ = 1.000 g/mL) at 20 °C. Specific volumes (V) ranging from 0.718 to 0.749 mL/g and $s^0_{20,w}$ of 2.6 S have been published (Ohlsson & Olsson, 1974; Baugh & Travis, 1976). Substitution of these values into the Svedberg equation (Svedberg & Pedersen, 1940) provided estimates for D of 0.898 and 1.009×10^{-6} cm^2 s^{-1}, respectively (mean, 0.954×10^{-6} cm^2 s^{-1}). By comparison, pancreatic chymotrypsinogen, which has a similar MW and a high degree of homology with HLE, has a diffusion coefficient of 0.95×10^{-6} s^{-1} (Wilcox et al., 1957).

General Method for Diffusion Kinetics Analysis. We wished to model local concentrations of HLE near the site of azurophil granule release and to compare predictions from this model to observational data. In an experimental system that we have recently used (Liou and Campbell, submitted for publication), PMN adhere tightly to a subjacent surface, and azurophil granules are extruded into the closed space between the adherent cell itself and the underlying surface. HLE can be considered to diffuse radially away from the extrusion site.

Since their formulation, the Fick diffusion equations (Fick, 1855) have been solved for a large number of geometries; two solutions of the Fick diffusion equations that closely approximate the diffusion of HLE describe diffusion of a substance from a disk source into a space defined by parallel planes extending from each flat disk surface. One solution (Crank, 1975)

$$C(r,t) = \frac{C_0}{2Dt} e^{-r^2/4Dt} \int_0^a e^{-r'^2/4Dt} I_0\left(\frac{rr'}{2Dt}\right) r' dr'$$

defines concentration, C, as a function of radius, r, from the center of the diffusion source, and time, t, after the diffusing process begins. The variable of integration is r'. The function I_0 is the modified Bessel function of the first kind, of order zero. Constants are as follows: a is the radius of the source, D is the diffusion coefficient, and C_0 is the concentration uniformly present in the original azurophil granule. We took a to be the geometric mean radius of the azurophil granule, 0.171 μm, and the diffusion coefficient for HLE to be 0.954×10^{-6} cm^2 s^{-1}. Although there is no symbolic solution to this equation (Crank, 1975), numerical solutions are readily available.

Numerical Analysis of C(r,t). Using Mathcad 4.0 from Mathsoft (Cambridge, MA), we directly calculated $C(r,t)$ for every 1 ms increment from 1 ms to 1.0 s following degranulation and for each radius between 0 and 15 μm in 0.01 μm increments. This numerical analysis created a 1000 × 1500 solution matrix, consisting of 1.5×10^6 elements. By considering the calculated data at particular times and radii, we constructed families of solutions referenced to time and space.

Because C depends on two variables, our results showing the concentration behavior of HLE in space and time are themselves three dimensional. However, we have chosen to present two-dimensional representations that are more easily shown and understood and that allow emphasis of specific spatial or temporal features of the full solution. For example, by presenting families of curves representing C at particular times or places, we can provide information from the full three-dimensional representation while retaining the selected feature of emphasis.

Changes in HLE Concentration with Time Following Degranulation. Figure 1 shows the changes with time in the calculated concentration of HLE at six different radii. Note that, at each radius depicted, a clearly definable maximum concentration of HLE is reached. When the measurement point is quite near to the site of degranulation, there is a very early and steep rise in predicted enzyme concentration, followed by a somewhat more gradual fall. At greater distances from the site of degranulation, a slower rise and a slower fall are predicted, along with a progressively more delayed attainment of the peak concentration.

The solution matrix from which the data in Figure 1 were extracted allows determination of the duration for which the predicted HLE concentration will exceed a specified value at any given radius. For example, the normal plasma

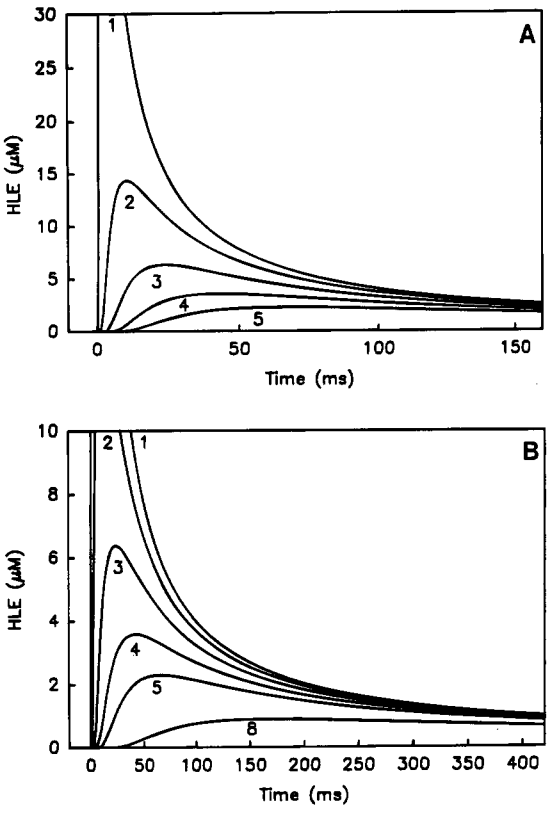

FIGURE 1: HLE concentration at various radii as a function of time. Each of the curves describes this relationship at a specific distance from the site of granule extrusion. Each curve is labeled with a number representing distance (μm) from the center of the site of degranulation. The time course of the local HLE concentration varies strikingly over short distances. Panels A and B display vertical scales that are relevant for normal and α_1-antitrypsin-deficient individuals, in whom mean plasma concentrations of α_1-antitrypsin are 32.8 and 5.3 μM, respectively. See text for analysis and clinical significance.

concentration of α_1-antitrypsin, the major circulating inhibitor of HLE, is 32.8 μM (Brantly et al., 1991). At a radius of 1 μm, the predicted HLE concentration exceeds that of α_1-antitrypsin in normal plasma for 8.6 ms. In contrast, this concentration is not reached at all at a radius of 2 μm. It is instructive to repeat this analysis for an HLE concentration of 5.3 μM, the mean plasma concentration of α_1-antitrypsin in individuals with the most prevalent type (Pi Z) α_1-antitrypsin deficiency (Brantly et al., 1991). The predicted HLE concentration exceeds the latter value for 74.2 ms at a radius of 2 μm and exceeds this value for 33.0 ms at a radius of 3 μm. Thus, the data in Figure 1 demonstrate that obligate catalytic activity of HLE (excess of local enzyme over local inhibitor concentration) is normally tightly confined in both space and time but that the extracellular volume containing active enzyme (and the time for which obligate activity is sustained) must necessarily increase in individuals who have α_1-antitrypsin deficiency.

Changes in HLE Concentration as a Function of Radius from Site of Degranulation. Figure 2A shows a subset of the family of curves relating HLE concentration to the radius at which it is measured (eight different observation times are shown). As expected, high concentrations are observed only for short time intervals after degranulation and only for small radii.

With study of Figure 2A, it becomes apparent that, for any given HLE concentration, a single curve will contain the maximal radius for which that concentration is achieved. Curves for a large number of time intervals can also be plotted, as in Figure 2B, which contains data for 29 points in time ranging from 1 to 400 ms.

Comparing Figure 2A with Figure 2B leads to a critically important concept regarding diffusion events near the site of granule extrusion. It is apparent that all possible solutions of $C(r,t)$ lie within a clearly defined boundary. This concept is confirmed numerically by the 1.5-million-element solution matrix that we derived by numerical analysis as described above. This boundary indicates that a single maximum radius exists for any chosen concentration of HLE. In our solution matrix for $C(r,t)$, we were able to choose the maximal radius at which each included concentration of HLE is found. These points form a smooth curve (Figure 2C) and describe the boundary that is apparent in Figure 2B. Thus, data from all time points fill the area below and to the left of this envelope curve, and no possible combination of concentration and radius lies upward and to the right of the curve.

Since the envelope curve in Figure 2C shows the maximum radius for which a given concentration of HLE is reached at any time following degranulation, it can be used to predict the maximum radius for which obligate catalytic activity will occur (i.e., the maximum radius within which the ratio of enzyme:inhibitor will exceed 1:1 for *some period of time*), for any given concentration of extracellular inhibitor(s). For a normal physiologic concentration of α_1-antitrypsin, 32.8 μM, the predicted radius is 1.33 μm. The radius increases 2.5-fold, to 3.3 μm, when the average deficient concentration of inhibitor, 5.3 μM (Brantly et al., 1991), is present in the bathing medium.

Further analysis of the markedly curvilinear relationship in Figure 2C indicates that it displays only slight curvature above a concentration of 10 μM. Below that value, however, minor decreases in concentration are associated with progressively greater increments in radius. The function reaches its maximum curvature at 2.25 μM.

Concurrence of Predictions with Observations. When PMN are allowed to spread on a fibronectin-coated surface under specific conditions and with varying concentrations of several inhibitors in the bathing medium (Liou and Campbell, submitted for publication), we have been able to image rounded areas of degraded substrate that represent the residua of quantum bursts of proteolytic activity. HLE was confirmed as the proteolytic agent by use of an HLE-specific inhibitor, ICI 200 355 which reproduced the results with α_1-antitrypsin (Liou and Campbell, submitted for publication). We hypothesized that the radii of the discrete zones of degraded fibronectin reflected radii of obligate catalytic activity of HLE, in which the enzyme concentration exceeded pericellular inhibitor concentrations. To test this hypothesis, we superposed experimental data from our imaging experiments (Liou and Campbell, submitted for publication) upon the envelope curve displayed in Figure 2C.

Figure 2D shows remarkably good agreement between the prediction and observations, with four different inhibitors and over a wide range of inhibitor concentrations. Of the 77 data points shown, 54 have 95% confidence intervals that include the theoretical prediction. Of the 23 points that do not have confidence intervals that include the theoretical prediction, 20 were obtained at inhibitor concentrations below 2 μM or above 40 μM, suggesting that the model has excellent predictive value within the range of concentrations

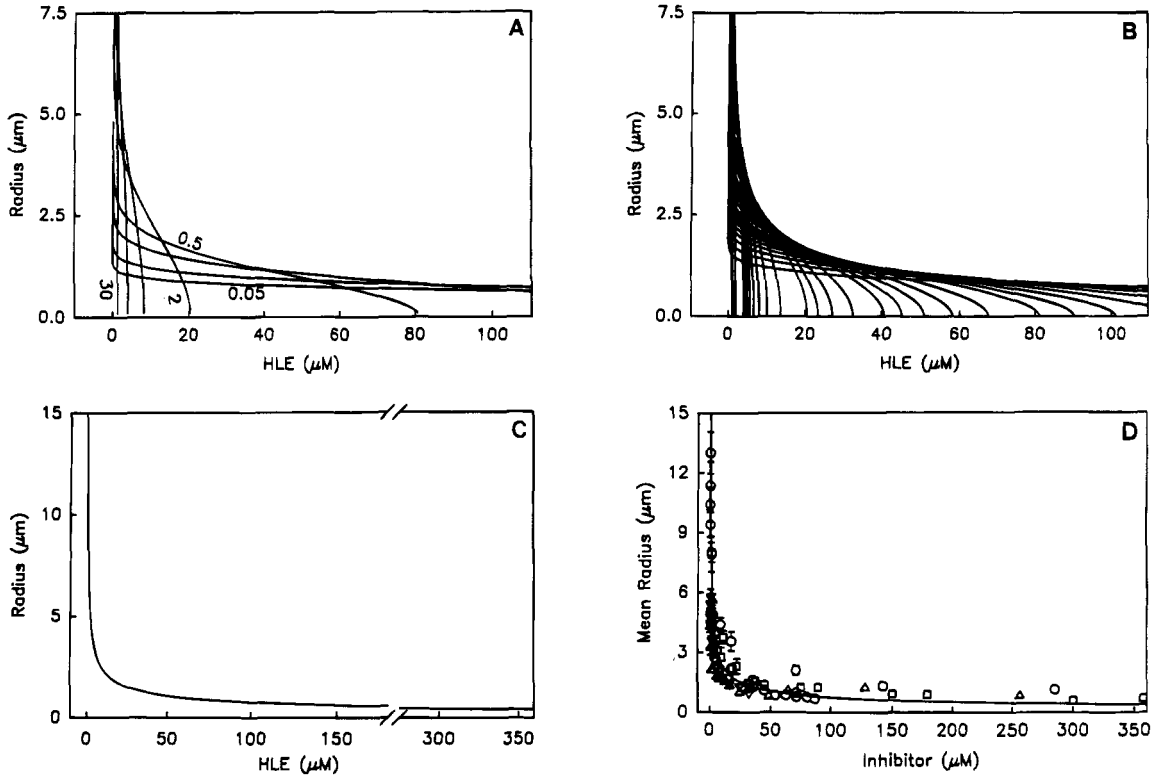

FIGURE 2: Relationship of radius of diffusion to local HLE concentration. In panel A, each of the curves describes this relationship at a specific interval following granule extrusion. The numbers adjacent to selected curves denote time in hundredths of seconds; the various curves are 0.05, 0.10, 0.25, 0.5, 2.0, 4.0, 7.0, and 30 ($\times 10^{-2}$ s). In panel B, 21 additional curves have been added to panel A. The curves now span a time from 1 to 400 ms after a degranulation, and they demonstrate clearly that there is a unique maximum radius at which an arbitrarily chosen concentration of HLE can be found. Note that all data points fall in the area below and to the left of a clearly definable boundary. Panel C shows a curve enveloping all members of the family of curves in panels A and B. No values of $C(r,t)$ can fall above and to the right of this envelope curve. Note the strikingly curvilinear relationship between the distance from the site of degranulation and the maximum HLE concentration that is achieved (at any time) at that radius. See text for explanation of significance. Panel D provides a superposition of observational data upon predicted local HLE concentrations. The data points are derived from direct observations (Liou and Campbell, submitted for publication) of the size of PMN-derived quantum proteolytic events occurring in various concentrations of bathing inhibitors. Circles, squares, and upward- and downward-pointing triangles represent experiments in which α_1-antitrypsin, ICI 200 355, recombinant secretory leukoprotease inhibitor, and α_2-macroglobulin, respectively, were the inhibitors surrounding the cells. Symbols represent mean radii; error bars are standard errors of the means. Where error bars are not seen, they are obscured by the symbol. The solid curve is the local maximal HLE concentration predicted from panel C. The outer edge of the quantum proteolytic events occured at the radii where the predicted local maximal HLE concentrations matched that of the inhibitors in the bathing medium, for each of the four inhibitors.

found in human serum for α_1-antitrypsin. The concordance of predictions with experimentation, especially over the physiologic range, indicates that the local ratio of enzyme: inhibitor provided the dominant effect on the size of local proteolytic lesions and that enzyme−inhibitor interactions are rapid in relation to diffusion times with the inhibitors tested.

Validation of Intragranular HLE Concentration. Because the shape and position of the envelope function are highly sensitive to intragranular HLE concentration, Figure 2C also provides an observational test of the very high initial HLE concentration (C_0) that we calculated from first principles. To explore the range of reasonable values for C_0, we generated a family of envelope functions by recalculation of $C(r,t)$ using a range of values for C_0 and then fit the functions to our observational data. Values of C_0 in the range of 1−10 mM resulted in envelope functions that fit the data acceptably (not shown). Values of C_0 outside this range resulted in envelope functions that clearly diverged from the experimental data.

Changes in Maximal HLE Concentration as a Function of Time Following Degranulation. To find the maximum duration for which any HLE concentration is sustained, we constructed another function from our numerical analyses (Figure 3) to emphasize concentration−time relationships. This function is also strikingly curvilinear, reaching its

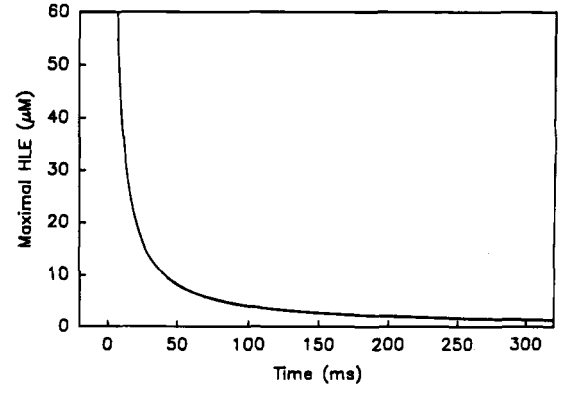

FIGURE 3: Maximal HLE concentration as a function of time. Because diffusion occurs only down gradients, the maximal HLE concentration at any time is always at $r = 0$ μm. For this special case, $C(0,t)$ can be symbolically evaluated (Crank, 1975) as $C = C_0[1 - e^{-a^2/(4Dt)}]$. We can plot this function directly or after numerical analysis of $C(r,t)$. Note that HLE concentrations less than ~10 μM are sustained for markedly increasing durations.

greatest curvature when the maximal concentration of HLE is 0.63 μM. This relationship shows that high concentrations of HLE are sustained for only brief periods, whereas concentrations lower than 10 μM are sustained for exponentially increasing durations.

Obtaining direct experimental data by imaging PMN during quantum proteolysis on a millisecond time scale remains a technically challenging goal, so the predictions shown in Figure 3 provide information that cannot be learned from observation at present. The relationship shown in Figure 3 clearly indicates that concentrations of HLE higher than 30 μM persist for less than 14 ms whereas concentrations of less than 10 μM persist for greater than 40 ms. For example, 32.8 μM HLE persists for 12.4 ms, whereas 5.3 μM HLE persists for 77.1 ms.

DISCUSSION

In this report, we have provided a robust method for modeling the rapidly changing local concentrations of HLE following release of azurophil granules into the cleft subjacent to an adherent PMN *in vitro*. An exceptional strength of this system is that it has allowed us to test predictions by comparison with our recent direct observations of PMN (Liou and Campbell, submitted for publication). The concordance of the predictions and observations validates the novel concept that microenvironments containing proteinases with obligate catalytic activity must exist in the zones surrounding sites of granule extrusion. In these zones, which are of definable size and duration, obligate catalytic activity of released proteinases exists despite the presence of proteinase inhibitors in the surrounding milieu. At a minimum, the present concepts and results provide a new perspective on enzyme−inhibitor interactions in biologic systems and a novel construct for understanding tissue injury in α_1-antitrypsin deficiency.

Contents and Geometry of PMN Azurophil Granules. During specific phases of the maturation of inflammatory cells in the bone marrow, a variety of constituents are synthesized and stored in cytoplasmic granules (Henson et al., 1992). HLE, for example, is synthesized during the promyelocytic and promonocytic stages of differentiation of PMN and monocytes, respectively, and packaged into azurophil granules of the maturing cells (Takahashi et al., 1988). After release from the bone marrow, mature PMN do not synthesize HLE, but they are capable of rapidly mobilizing azurophil granules to the cell surface in response to varied stimuli (Henson et al., 1992).

To begin to understand local concentrations of HLE that are achievable *in vivo*, we have made several calculations from first principles. From the electron microscopic morphometry of PMN and immunoassays of the cells' content of HLE, we calculated that azurophil granules contain a very high concentration of HLE (5.33 mM) in a very small volume (2.09×10^{-17} L). Thus, although each azurophil granule contains only approximately 67 000 molecules of HLE, the intragranular concentration of enzyme is nearly 3 orders of magnitude greater than the concentration of elastase inhibitors that normally bathes the cells *in vivo* (Travis & Salvesen, 1983; Brantly et al., 1991). *In vitro* kinetic studies of substrate catalysis by such high concentrations of HLE would be quite challenging. We have found, for example, that cleavage of methoxysuccinyl-Ala-Ala-Pro-Val *p*-nitroanilide (100 μM) by 4 μM HLE is more than 75% complete within 1 s (Liou and Campbell, unpublished observations). Note that this concentration of HLE is ~3 orders of magnitude *lower* than that of the intragranular enzyme.

The calculations of granule volume and intragranular enzyme concentration are straightforward and based upon sound primary observations. We chose to use our own measurements (Campbell et al., 1989) of the amount of HLE per cell (1.11 ± 0.11 pg; $n = 15$ subjects) rather than the similar result (1.59 pg) of Damiano et al. (1988) because our result provided a more conservative calculation than Damiano's and because his value was based upon study of only five individuals. We used results of Damiano's morphometry of azurophil granules (Damiano et al., 1988), which are the most recent and rigorous but which agree reasonably well with earlier studies by Bainton et al. (1971).

Azurophil granules also contain cathepsin G and proteinase 3 in amounts similar to that of HLE (Campbell et al., 1989; Egesten et al., 1994). However, work from this and other laboratories (Campbell et al., 1982; Campbell & Campbell, 1988; Chamba et al., 1991; Liou and Campbell, submitted for publication) indicate that PMN-mediated proteolysis of many extracellular substrates, including fibronectin, is mediated largely or entirely by activity of HLE. Thus, the analysis reported herein has focused exclusively upon HLE.

Quantum Bursts of Proteolytic Activity. The simulations reported herein, and our recent direct experimentation (Liou and Campbell, submitted for publication), support the concept that PMN-derived proteolysis *in vivo* (in the presence of proteinase inhibitors) normally occurs in brief quantum bursts. For example, if PMN are bathed in HLE inhibitors at normal plasma levels, obligate catalytic activity of HLE *must* exist until the enzyme:inhibitor ratio falls to <1:1. It is reasonable to hypothesize that millimolar or even micromolar concentrations of enzyme would very rapidly occupy essentially all available substrate binding sites in the pericellular zone. Subsequently, catalytic activity of any residual free enzyme will be extinguished, although enzyme bound to substrate may have continued activity (Bruch & Bieth, 1986; Morrison et al., 1990).

Proteinase Inhibitors Confine Quantum Bursts of Catalytic Activity. Our simulations and observations indicate that extracellular inhibitors, in concentrations that exist *in vivo*, *confine*, but cannot eliminate, activity of HLE; moreover, we can estimate the radius (or volume of fluid) that *must* contain active enzyme following granule release. For example, Figure 2B reveals that, in the presence of normal plasma α_1-antitrypsin concentrations (Travis & Salvesen, 1983; Brantly et al., 1991), HLE will exceed inhibitor concentration, and therefore remain active, up to 1.33 μm from the site of granule extrusion (7.8 times the mean radius of an azurophil granule), and for 12.4 ms.

Inspection of the shape of the relationship in Figure 2B indicates that higher inhibitor concentrations will produce modest, but potentially significant, additional confinement of the catalytic activity. Thus, the acute-phase response of α_1-antitrypsin to injury, infection, or inflammation may serve an important role in reducing tissue injury during a period of increased PMN extravasation. Conversely, if the local concentration of active inhibitors is reduced—for example, by oxidative inactivation (Weiss, 1989)—the radius and duration of obligate catalytic activity will be increased.

Finally, our simulations underscore the importance of the ability of PMN to adhere in close proximity to extracellular substrates. In the presence of physiologic concentrations of

extracellular inhibitors, it is primarily substrates that lie within a few microns of the PMN cell surface that are at risk. Similarly, to the extent that active HLE may exert juxtacrine effects on other cells (Sommerhoff et al., 1990; Hubbard et al., 1991; Fahy et al., 1992; Nakamura et al., 1992), the range over which this effect is exerted is a few microns.

Relationship to Other Mechanisms of Local Protein Degradation. Even in the presence of proteinase inhibitors, PMN and other cells have the potential to degrade extracellular proteins through several mechanisms that include (1) high local concentrations of enzyme (the subject of this report); (2) local inactivation of proteinase inhibitors (Desrochers et al., 1991, 1992; Vissers et al., 1988; Weiss, 1989; Reddy et al., 1994); (3) membrane-bound enzymes (Bangalore & Travis, 1994; Owen et al., 1995); and (4) persistent binding of enzyme to substrate (Bruch & Bieth, 1986; Morrison et al., 1990; Kolev et al., 1994). Among these mechanisms, substantial attention has focused upon the ability of superoxide anion, myeloperoxidase, and reactive species derived from myeloperoxidase activity to oxidatively inactivate proteinase inhibitors (Carp & Janoff, 1980; Vissers et al., 1985; Weiss, 1989; Reddy et al., 1994). One or more of the above mechanisms may be important during various inflammatory events *in vivo*, but in our direct observations of quantum proteolytic events *in vitro*, locally high proteinase concentrations have exerted a dominant effect.

Implications for α_1-Antitrypsin Deficiency. α_1-Antitrypsin deficiency is the most prevalent potentially lethal hereditary disease of adult Caucasians (Silverman et al., 1989; Troyer et al., submitted for publication). Individuals with the Pi Z phenotype, who express only the abnormal Z variant of the protein, have by far the most common type of α_1-antitrypsin deficiency (Brantly et al., 1988). These individuals have circulating α_1-antitrypsin levels that are 10−15% of normal and have a markedly increased risk of developing early-onset, severe pulmonary emphysema, particularly if they smoke (Hutchison, 1988). The lung parenchymal injury is consistent with defective inhibition of HLE in these individuals, since α_1-antitrypsin is thought to be the most important inhibitor of HLE in the lower respiratory tract (Gadek et al., 1981; Travis & Salvesen, 1983). However, two critical issues that cloud this hypothesis are inadequately addressed by classical kinetic analyses: (1) α_1-antitrypsin is a fast-acting pseudo-irreversible inhibitor of HLE with $K_i \sim 10^{-14}$ M (Beatty et al., 1984), so the levels of α_1-antitrypsin even in deficient individuals exceed the K_i for HLE by over 7 orders of magnitude; and (2) heterozygotes for α_1-antitrypsin deficiency who have the Pi SZ phenotype have α_1-antitrypsin levels that are a mean of 50.3% of normal (Brantly et al., 1991), yet in marked contrast to Pi Z individuals they suffer minimal if any increased risk of tissue injury (Hutchison, 1988).

The present work provides novel insights into the paradox posed by the above issues. Our data indicate that the reduction in α_1-antitrypsin concentrations to levels seen in α_1-antitrypsin deficiency is alone sufficient to increase the radius of quantum proteolytic events by 2.5-fold and the duration of catalytic activity in the local microenvironment by 6.2-fold, even if the normal and the Z variants had identical kinetics of enzyme inhibition (Adams & Hamliton, 1984; Ogushi et al., 1987). In contrast, because of the markedly curvilinear relationships, and the location of the areas of greatest curvature of the data shown in Figures 2C and 3, variations in α_1-antitrypsin concentrations above 10−20 μM (as seen in heterozygotes) result in much smaller changes.

On purely empiric grounds, the clinical concept of a "protective threshold concentration" of α_1-antitrypsin has been developed (Wewers et al., 1987; Buist et al., 1989). Only individuals with α_1-antitrypsin levels below this concentration are considered to have an excess risk of lung injury. The standard clinical practice for therapy of selected patients with α_1-antitrypsin deficiency is to augment their α_1-antitrypsin levels by periodic intravenous infusions of purified inhibitor (Buist et al., 1989). The dose and the dosing interval have been chosen to achieve and sustain plasma levels of α_1-antitrypsin greater than the threshold value. It is of interest that the threshold value of α_1-antitrypsin determined on clinical grounds is 80 mg/dL, or $\sim$11 μM when analyzed against standards of purified α_1-antitrypsin (Brantly et al., 1991). Examination of Figures 2C and 3 reveals that this value lies at the inhibitor concentration below which the radius and duration of obligate activity of released HLE begin to increase markedly. Thus, our model provides a scientific basis for the clinical concept of a protective threshold concentration of α_1-antitrypsin and provides insights into the pathogenesis of tissue injury in α_1-antitrypsin deficiency that could not have been anticipated from traditional enzyme kinetics analyses.

Applicability of Nonisotropic Modeling to Other Systems. The importance of our simulations transcends the specific topic of quantum proteolysis by PMN. Other enzyme and nonenzyme granule contents of PMN are also released in small quanta at high concentrations. Other inflammatory cells, including eosinophils, basophil/mast cells and monocytes also contain granules that are released into the extracellular space in response to varied signals. Given appropriate constants that can be easily learned, similar simulations that closely mimic other cellular systems may be straightforward. For systems where the local geometry is complicated, however, such simulations are more difficult. For example, a previous study that simulated the diffusion of acetylcholine in two dimensions (Wathey et al., 1979), in an attempt to model miniature end-plate potentials, was criticized for only roughly approximating diffusion in the complicated three-dimensional neuromuscular junction (Bartol et al., 1991).

The concepts arising from the present work have applicability to a variety of settings in the biological world. Secretion of a wealth of products from noninflammatory cells must be viewed in the context of their local concentrations at the site of release, and short-range juxtacrine effects of such products should be envisaged in terms of their concentrations in the local tissue environment.

There are rich opportunities for extending these simulations. As HLE diffuses away from the site of degranulation, traditional enzyme kinetics can be integrated into the diffusion analysis to assess the delay time of inhibition more precisely. We can also simulate geometries other than those that exist when PMN are tightly applied to a planar surface. For example, when the cells are in suspension rather than adherent to a surface, local enzyme concentrations follow a different pattern in time and space (Liou and Campbell, unpublished data). The simulations presented herein already mandate new concepts of the cell biology of neutrophils,

provide new insights into α_1-antitrypsin deficiency, and have important implications for therapeutics of diseases associated with tissue injury during inflammation. Finally, we are introducing a new diffusion-based nonisotropic paradigm for enzyme kinetics that applies to any enzyme and may have implications for reaction kinetics that applies to any signaling molecule that is released in highly concentrated packets.

ACKNOWLEDGMENT

We wish to thank David J. Bird (University of Illinois, Urbana−Champaign) and Brian E. Fick (Fermi Institute, University of Chicago) for helpful discussions and John R. Hoidal (University of Utah), Charles Grissom (University of Utah), and Mitchell Glass (Zeneca Pharmaceuticals) for critical reviews of the manuscript.

REFERENCES

Adams, D. O., & Hamilton, T. A. (1984) *Annu. Rev. Immunol. 2*, 283−318.
Bainton, D. F., Ullyot, J. L., & Farquhar, M. G. (1971) *J. Exp. Med. 134*, 907−934.
Bangalore, N., & Travis, J. (1994) *Biol. Chem. Hoppe-Seyler 375*, 659−666.
Bartol, M. B., Jr., Land, B. R., Salpeter, E. E., & Salpeter, M. M. (1991) *Biophys. J. 59*, 1290−1307.
Baugh, R. J., & Travis, J. (1976) *Biochemistry 15*, 836−841.
Beatty, K., Matheson, N., & Travis, J. (1984) *Hoppe-Seyler's Z. Physiol. Chem. 365*, 731−736.
Bieth, J. G. (1980) *Bull. Eur. Physiopathol. Respir. 16*, (Suppl.), 183−195.
Bieth, J. G. (1986) in *Biology of Extracellular Matrix: Regulation of Matrix Accumulation* (Mecham, R. P., Ed.) pp 217−320, Academic Press, Inc., Orlando.
Brantly, M., Nukiwa, T., & Crystal, R. G. (1988) *Am. J. Med. 84*, 13−31.
Brantly, M. L., Wittes, J. T.; Vogelmeier, C. F., Hubbard, R. C., Fells, G. A., & Crystal, R. G. (1991) *Chest 100*, 703−708.
Bruch, M., & Bieth, J. G. (1986) *Biochem. J. 238*, 269−273.
Buist, A. S., Burrows, B., Cohen, A., Crystal, R. G., Fallat, R. J., Gadek, J. E., & Turino, G. M. (1989) *Am. Rev. Respir. Dis. 140*, 1494−1497.
Campbell, E. J., & Campbell, M. A. (1988) *J. Cell Biol. 106*, 667−676.
Campbell, E. J., Senior, R. M., McDonald, J. A., & Cox, D. L. (1982) *J. Clin. Invest. 70*, 845−852.
Campbell, E. J., Silverman, E. K., & Campbell, M. A. (1989) *J. Immunol. 143*, 2961−2968.
Carp, H., & Janoff, A. (1980) *J. Clin. Invest. 66*, 987−995.
Chamba, A., Afford, S. C., Stockley, R. A., & Burnett, D. (1991) *Am. J. Respir. Cell Mol. Biol. 4*, 330−337.
Crank, J. (1975) in *The Mathematics of Diffusion*, 2nd ed., Chapter 3, pp 28−43, Oxford University Press, New York.
Crystal, R. G., Brantly, M. L., Hubbard, R. C., Curiel, D. T., States, D. J., & Holmes, M. D. (1989) *Chest 95*, 196−206.
Damiano, V. V., Kucich, U., Murer, E., Laudenslager, N., & Weinbaum, G. (1988) *Am. J. Pathol. 131*, 235−245.
Desrochers, P. E., Jeffrey, J. J., & Weiss, S. J. (1991) *J. Clin. Invest. 87*, 2258−2265.
Desrochers, P. E., Mookhtiar, K., Van Wart, H. E., Hasty, K. A., & Weiss, S. J. (1992) *J. Biol. Chem. 267*, 5005−5012.
Egesten, A., Breton-Gorius, J., Guichard, J., Gullberg, U., & Olsson, I. (1994) *Blood 83*, 2985−2994.
Fahy, J. V., Schuster, A., Ueki, I., Boushey, H. A., & Nadel, J. A. (1992) *Am. Rev. Respir. Dis. 146*, 1430−1433.
Fick, A. (1855) *Ann. Phys. Chem. 94*, 59−86.
Gadek, J. E., Fells, G. A., Zimmerman, R. L., Rennard, S. I., & Crystal, R. G. (1981) *J. Clin. Invest. 68*, 889−898.
Havemann, K., & Janoff, A. (1978) in *Neutral Proteases of Human Polymorphonuclear Leukocytes*, Urban and Schwartzenberg, Baltimore and Munich.
Henson, P. M., Henson, J. E., Fittschen, C., Bratton, D. L., & Riches, D. W. H. (1992) in *Inflammation: Basic Principles and Clinical Correlates* (Gallin, J. I., Goldstein, I. M., & Snyderman, R., Eds.) pp 511−539, Raven Press, Ltd., New York.
Hubbard, R. C., & Crystal, R. G. (1991) in *The Lung: Scientific Foundations* (Crystal, R. G., & West, J. B., Eds.) pp 2059−2072, Raven Press, Ltd., New York.
Hubbard, R. C., Sellers, S., Czerski, D., Stephens, L., & Crystal, R. G. (1988) *J. Am. Med. Assoc. 260*, 1259−1264.
Hubbard, R. C., Fells, G., Gadek, J., Pacholok, S., Humes, J., & Crystal, R. G. (1991) *J. Clin. Invest. 88*, 891−897.
Hutchison, D. C. S. (1988) *Am. J. Med. 84*, 3−12.
Kolev, K., Lerant, I., Tenekejiev, J., & Machovich, R. (1994) *J. Biol. Chem. 269*, 17030−17034.
Morrison, H. M., Welgus, H. G., Stockley, R. A., Burnett, D., & Campbell, E. J. (1990) *Am. J. Respir. Cell Mol. Biol. 2*, 263−269.
Nakamura, H., Yoshimura, K., McElvaney, N. G., & Crystal, R. G. (1992) *J. Clin. Invest. 89*, 1478−1484.
Ogushi, F., Fells, G. A., Hubbard, R. C., Straus, S. D., & Crystal, R. G. (1987) *J. Clin. Invest. 80*, 1366−1374.
Ohlsson, K., & Olsson, I. (1974) *Eur. J. Biochem. 42*, 519−527.
Owen, C. A., & Campbell, E. J. (1995) in *Adult Respiratory Distress Syndrome* (Haslett, C., & Evans, T., Eds.) Chapman & Hall, London.
Owen, C. A., Campbell, M. A., Sannes, P. L., Boukedes, S. S., & Campbell, E. J. (1995) *J. Cell Biol. 131*, 775−789.
Reddy, V. Y., Desrochers, P. E., Pizzo, S. V., Gonias, S. L., Sahakian, J. A., Levine, R. L., & Weiss, S. J. (1994) *J. Biol. Chem. 269*, 4683−4691.
Rice, W. G., & Weiss, S. J. (1990) *Science 249*, 178−181.
Silverman, E. K., Miletich, J. P., Pierce, J. A., Sherman, L. A., Endicott, S. K., Broze, G. J., & Campbell, E. J. (1989) *Am. Rev. Respir. Dir 140*, 961−966.
Sommerhoff, C. P., Nadel, J. A., Basbaum, C. B., & Caughey, G. H. (1990) *J. Clin. Invest. 85*, 862−869.
Svedberg, T., & Pedersen, K. O., Eds. (1940) *The Ultracentrifuge*, Oxford University Press, London.
Takahashi, H., Nukiwa, T., Basset, P., & Crystal, R. G. (1988) *J. Biol. Chem. 263*, 2543−2547.
Travis, J., & Salvesen, G. S. (1983) *Annu. Rev. Biochem. 52*, 655−709.
Vissers, M. C. M., Day, W. A., & Winterbourn, C. C. (1985) *Blood 66*, 161−166.
Vissers, M. C. M., George, P. M., Bathurst, I. C., Brennan, S. O., & Winterbourn, C. C. (1988) *J. Clin. Invest. 82*, 706−711.
Wathey, J. C., Nass, M. M., & Lester, H. A. (1979) *Biophys. J. 27*, 145−164.
Weiss, S. J. (1989) *N. Engl. J. Med. 320*, 365−376.
Wewers, M. D., Casolaro, M. A., Sellers, S. E., Swayze, S. C., McPhaul, K. M., Wittes, J. T., & Crystal, R. G. (1987) *N. Engl. J. Med. 316*, 1055−1062.
Wilcox, P. E., Kraut, J., Wade, R. D., & Neurath, H. (1957) *Biochim. Biophys. Acta 24*, 72−78.

BI951138A